Simulation of Moisture Loss and Heat Loads in Refrigerated Storage of Fruits and Vegetables

Bryan R. Becker, Ph.D. and Brian A. Fricke[1]

ABSTRACT

A computer algorithm was developed which estimates the latent and sensible heat loads as well as the commodity moisture loss and temperature distribution which occurs during the bulk refrigeration of fruits and vegetables. This paper discusses commodity thermophysical properties and flowfield parameters which govern the heat and mass transfer from fruits and vegetables. Commodity thermophysical properties include transpiration and respiration, while flowfield parameters include psychrometric properties and convective heat and mass transfer coefficients. In addition, the modeling treatment of these properties and parameters is described. This paper discusses the modeling methodology utilized in the current computer algorithm and describes the development of the heat and mass transfer models. This paper also compares the results of the computer algorithm to experimental data taken from the literature. Existing bulk load heat transfer models are also reviewed.

Keywords. Computer simulation, Bulk storage, Fresh fruits and vegetables, Transpiration, Respiration

INTRODUCTION

The storage life of a commodity is drastically affected by the temperature and humidity of its surroundings. Precooling has long been known to effectively retard ripening and control microbial processes (Baird and Gaffney, 1976). The refrigeration of fruits and vegetables retards respiratory heat generation, wilting due to moisture loss, and spoilage caused by the invasion of bacteria, fungi and yeasts. Refrigeration also retards undesirable growth or sprouting by the commodity itself (USDA, 1986).

To ensure optimum commodity quality during refrigeration, the temperature and humidity of the conditioned air within the refrigerated facility must be precisely controlled. In order to properly design such a facility and its associated refrigeration equipment, the designer must estimate both the sensible and latent heat loads due to the stored commodity. This requires knowledge of the complex interaction of the various thermophysical processes which occur within and around fresh fruits and vegetables. These processes include convective heat and mass transfer as well as transpiration and respiration.

This paper describes a computer algorithm which was developed to aid in the design of bulk refrigeration facilities for fruits and vegetables. This computer model utilizes a porous media approach to estimate the latent and sensible heat loads due to the bulk refrigeration of fruits and vegetables. The combined phenomena of transpiration, respiration, air flow, and convective heat and mass transfer are included in the model. In addition to latent and sensible heat loads, the computer algorithm also predicts the commodity moisture loss which occurs during refrigeration and the temperature distribution within the commodity.

This paper describes the pertinent factors which govern the heat and mass transfer from fresh fruits and vegetables. These factors include both thermophysical properties of commodities as well as flowfield parameters. Accurate treatment of these various thermophysical properties and flowfield parameters is necessary to assure that the computer algorithm yields reasonable results. The present work describes this

[1]Bryan R. Becker, Ph.D., P.E. is an Associate Professor and Brian A. Fricke is a Research Assistant in the Mechanical and Aerospace Engineering Department, University of Missouri-Kansas City, 5605 Troost Avenue, Kansas City, MO 64110-2823.

treatment, which is based upon a thorough review of a wide variety of sources. In addition, this paper compares the results of the computer algorithm to experimental data taken from the literature. This paper also reviews existing numerical models for determining the heat transfer in bulk loads of fruits and vegetables.

A review of the literature has revealed several existing models of the heat transfer in the bulk refrigeration of fruits and vegetables. These models include those developed by Bakker-Arkema and Bickert (1966), Baird and Gaffney (1976), Adre and Hellickson (1989), Gan and Woods (1989), Talbot et al. (1990) and MacKinnon and Bilanski (1992). However, these models do not suitably fulfill the needs of the designers and operators of bulk refrigeration facilities. These models do not adequately address the effects of transpiration, respiration and evaporative cooling as well as temperature gradient within the commodity. In addition, these models do not estimate sensible and latent heat loads and they are not generalized to model a wide variety of commodities. Thus, the current computer algorithm was developed to estimate the latent and sensible heat loads as well as the moisture loss and temperature distribution in the bulk refrigeration of fruits and vegetables. This current computer algorithm is capable of modeling a wide variety of commodities.

THERMOPHYSICAL PROPERTIES OF COMMODITIES

The estimation of the mass and heat transfer which occurs in the bulk refrigeration of fruits and vegetables requires knowledge of various thermophysical properties of commodities. Mass transfer calculations require the determination of the transpiration rate which depends upon the air film mass transfer coefficient, the skin mass transfer coefficient and the vapor pressure lowering effect of the commodity. Heat transfer calculations require the determination of the heat generation due to respiration.

Transpiration

Transpiration is the moisture loss process exhibited by fresh fruits and vegetables. This process consists of the transport of moisture through the skin of the commodity, the evaporation of this moisture from the commodity surface and the convective mass transport of the moisture to the surroundings. The driving force for transpiration is a difference in water vapor pressure between the surface of a commodity and the surrounding air. Thus, the basic form of the transpiration model is given as follows:

$$\dot{m} = k_t (P_s - P_a) \tag{1}$$

where $\dot{m}$ 2 is the transpiration rate per unit area of commodity surface. In its simplest form, the transpiration coefficient, k_t, is considered to be a constant for a particular commodity. However, Fockens and Meffert (1972) modified the simple transpiration coefficient to model variable skin permeability and to account for air flow rate. Their modified transpiration coefficient takes the following form:

$$k_t = \frac{1}{\frac{1}{k_a} + \frac{1}{k_s}} \tag{2}$$

The air film mass transfer coefficient, k_a, describes the convective mass transfer which occurs at the surface of the commodity and is a function of air flow rate. The skin mass transfer coefficient, k_s, describes the skin's diffusional resistance to moisture migration.

Air Film Mass Transfer Coefficient

The air film mass transfer coefficient, k_a, can be estimated by using the Sherwood-Reynolds-

Schmidt correlations (Sastry and Buffington, 1982). The Sherwood number, *Sh*, is defined as follows:

$$\mathrm{Sh} = \frac{k_a d}{d} \tag{3}$$

where d is the diameter of the commodity and δ is the coefficient of diffusion of water vapor in air. For convective mass transfer from a spherical fruit or vegetable, Chau et al. (1987) recommended a Sherwood-Reynolds-Schmidt correlation of the form:

$$\mathrm{Sh} = 2.0 + 0.552\,\mathrm{Re}^{0.53}\mathrm{Sc}^{0.33} \tag{4}$$

which was taken from Geankoplis (1978). In the above equation, *Re* is the Reynolds number, $Re = u_\infty d/\nu$, and *Sc* is the Schmidt number, $Sc = \nu/\delta$, where u_∞ is the free stream air velocity and ν is the kinematic viscosity of air.

Skin Mass Transfer Coefficient

The skin mass transfer coefficient, k_s, which describes the resistance to moisture migration through the skin of a commodity, is based upon the fraction of the product surface covered by pores. Although it is difficult to theoretically determine the skin mass transfer coefficient, experimental determination has been performed by Chau et al. (1987) and Gan and Woods (1989). These experimental values of k_s are given in Table 1, along with estimated values of the skin mass transfer coefficient for grapes, onions, plums and potatoes. Note that three values of skin mass transfer coefficient are tabulated for most of the commodities. These values correspond to the spread of the experimental data.

Vapor Pressure Lowering Effect

In the absence of dissolved substances, the surface water vapor pressure, P_s, in Eq. 1, is the water vapor saturation pressure evaluated at the surface temperature of the commodity. However, dissolved substances, such as sugars, tend to lower the water vapor pressure at the surface of the commodity. Therefore, the water vapor pressure at the evaporating surface, P_s, becomes:

$$P_s = \mathrm{VPL} \bullet P_{ws}(T_s) \tag{5}$$

where *VPL* is the vapor pressure lowering effect of the commodity and $P_{ws}(T_s)$ is the water vapor saturation pressure evaluated at the surface temperature of the commodity, T_s. The vapor pressure lowering effect for various fruits and vegetables is given in Table 1 (Chau et al., 1987) while the water vapor saturation pressure is determined from psychrometric formulae.

Respiration

Respiration is the chemical process by which fruits and vegetables convert sugars and oxygen into carbon dioxide, water, and heat. The heat generated by the respiration process tends to increase the temperature of a commodity. This, in turn, increases the water vapor pressure just below the surface of the commodity, leading to increased transpiration (Sastry et al., 1978).

During the respiration process, sugar and oxygen are combined to form carbon dioxide, water and heat as follows:

$$C_6H_{12}O_6 + 6\ O_2 \rightarrow 6\ CO_2 + 6\ H_2O + 2667\ \mathrm{kJ} \tag{6}$$

The rate at which this chemical reaction takes place has been found to vary with the type and temperature of the commodity. In the present work, correlations were developed, based upon data given by the USDA

(1986), which relate a commodity's carbon dioxide production rate to its temperature. The carbon dioxide production rate can then be related to the heat generation due to respiration.

The resulting carbon dioxide production correlations are of the following form:

$$\dot{m}_{CO2} = f \bullet \left(\frac{9T_m}{5} + 32 \right)^g \tag{7}$$

where $\dot{m}_{CO2}$ 8 is the carbon dioxide production per unit mass of commodity (mg/kg h), T_m is the mass average commodity temperature (°C) and f and g are respiration coefficients which are given in Table 1. The respiration coefficients f and g were obtained via a least-squares fit to the data published by the USDA (1986).

Table 1. Commodity skin mass transfer coefficient, vapor pressure lowering effect (VPL) and respiration coefficients.†

Product	Skin Mass Transfer Coefficient, k_s, g/(m²·s·MPa)			VPL	Respiration Coefficients	
	Low	Mean	High		f	g
Apples	0.111	0.167	0.227	0.98	5.687×10^{-4}	2.598
Blueberries	0.955	2.19	3.39	0.98	7.252×10^{-5}	3.258
Brussels	9.64	13.3	18.6	0.99	0.002724	2.573
Cabbage	2.50	6.72	13.0	0.99	6.080×10^{-4}	2.618
Carrots	31.8	156	361	0.99	0.05002	1.793
Grapefruit	1.09	1.68	2.22	0.99	0.003583	1.998
Grapes	--	0.4024	--	0.98	7.056×10^{-5}	3.033
Green Peppers	0.545	2.159	4.36	0.99	3.510×10^{-4}	2.741
Lemons	1.09	2.08	3.50	0.98	0.01119	1.774
Lima Beans	3.27	4.33	5.72	0.99	9.105×10^{-4}	2.848
Limes	1.04	2.22	3.48	0.98	2.983×10^{-8}	4.733
Onions	--	0.8877	--	0.98	3.668×10^{-4}	2.538
Oranges	1.38	1.72	2.14	0.98	2.805×10^{-4}	2.684
Peaches	1.36	14.2	45.9	0.99	1.300×10^{-5}	3.642
Pears	0.523	0.686	1.20	0.98	6.361×10^{-5}	3.204
Plums	--	1.378	--	0.98	8.608×10^{-5}	2.972
Potatoes	--	0.6349	--	0.98	0.01709	1.769
Snap Beans	3.46	5.64	10.0	0.99	0.003283	2.508
Sugar Beets	9.09	33.6	87.3	0.96	8.591×10^{-3}	1.888
Strawberries	3.95	13.6	26.5	0.99	3.668×10^{-4}	3.033
Swedes	--	116.6	--	0.99	1.652×10^{-4}	2.904
Tomatoes	0.217	1.10	2.43	0.99	2.007×10^{-4}	2.835

† A portion of this data is reproduced from Chau et al. (1987) and Gan and Woods (1989).

The chemical reaction, Eq. 6, indicates that for every 6 moles of carbon dioxide produced, there are 2667 kJ (2530 Btu) of heat generated. Thus, for every one milligram (3.527×10^{-5} oz.) of carbon dioxide produced, 10.7 joules (0.0101 Btu) of heat are generated (USDA, 1986). The rate of respiratory heat generation per unit mass of commodity, W (J/kg h), then becomes:

$$W = (10.7)(\dot{m}_{CO2}) \tag{8}$$

FLOWFIELD PARAMETERS

In addition to the thermophysical properties of commodities, the current modeling methodology requires various flowfield parameters. Mass transfer calculations require the evaluation of the water vapor pressure at the commodity surface and in the surrounding refrigerated air. Heat transfer calculations require determination of the effective heat transfer coefficient.

Water Vapor Saturation Pressure

In the current algorithm, the water vapor saturation pressure is used to determine the vapor pressure at the surface of the commodity which is required for the transpiration calculation. The water vapor saturation pressure is also used to calculate the water vapor pressure in the refrigerated air.

ASHRAE (1977) indicates that the water vapor saturation pressure can be determined using the following equation:

$$\begin{aligned}\log_{10}(P_{ws}) = {} & 10.79586(1-q) + 5.02808\log_{10}(q) \\ & + 1.50474 \times 10^{-4}(1-10^{-8.29692[1/q-1]}) \\ & + 0.42873 \times 10^{-3}(10^{4.76955(1-q)}-1) \\ & - 2.2195983\end{aligned} \tag{9}$$

where P_{ws} is the water vapor saturation pressure (atm), $? = 273.16/T_{a,absolute}$, and $T_{a,absolute}$ is the absolute air temperature (K).

Water Vapor Pressure in Refrigerated Air

The water vapor pressure in the refrigerated air, P_a, can be found as follows (ASHRAE, 1993):

$$P_a = \frac{Pw}{0.62198 + w} \tag{10}$$

where P is the air pressure and w is the refrigerated air humidity ratio. The humidity ratio, which is the ratio of the mass of water vapor in a sample of air to the mass of dry air in that sample, is a function of the dry bulb temperature and the wet bulb temperature of the refrigerated air (ASHRAE, 1993).

Effective Heat Transfer Coefficient

The heat transfer, Q, between the surface of a commodity and the surrounding refrigerated air consists of convection heat transfer and radiation heat transfer. In the present work, an effective heat transfer coefficient, h_{eff}, is used to account for both the convection and radiation heat transfer:

$$h_{eff} = h_{convection} + h_{radiation} \tag{11}$$

where $h_{convection}$ is the convection heat transfer coefficient and $h_{radiation}$ is the radiation heat transfer coefficient. The heat transfer, Q, between the commodity surface and the refrigerated air can then be written as follows:

$$Q = h_{eff} \; A_s \; (\; T_s - T_a \;) \tag{12}$$

where A_s is the commodity surface area, T_s is the commodity surface temperature and T_a is the refrigerated air temperature.

Convection Heat Transfer Coefficient

The convection heat transfer coefficient, $h_{convection}$, can be estimated by using the Nusselt-Reynolds-Prandtl correlations (Incropera and DeWitt, 1990). The Nusselt number, Nu, is defined as follows:

$$Nu = \frac{h_{convection} d}{k_{air}} \tag{13}$$

where $h_{convection}$ is the convection heat transfer coefficient, d is the diameter of the commodity and k_{air} is the thermal conductivity of air.

Since the convective heat transfer and convective mass transfer processes are governed by similar mechanisms, a Nusselt-Reynolds-Prandtl correlation can be formed which corresponds to the previously described Sherwood-Reynolds-Schmidt correlation given in Eq. 4. This can be accomplished by replacing the Sherwood number, *Sh*, and the Schmidt number, *Sc*, with the Nusselt number, *Nu*, and the Prandtl number, $Pr = \nu/\alpha$, respectively:

$$Nu = 2.0 + 0.552\, Re^{0.53} Pr^{0.33} \tag{14}$$

Radiation Heat Transfer Coefficient

In the present work, the radiation heat transfer coefficient, $h_{radiation}$, is determined by linearizing the radiation heat transfer equation. Assuming that the commodity is surrounded by refrigerated air and that it exhibits blackbody radiation, the following simplified form of the radiation heat transfer equation is obtained (Incropera and DeWitt, 1990):

$$Q_r = \sigma\, A_s (T_s^4 - T_a^4) \tag{15}$$

This equation can then be factored to yield the following form:

$$Q_r = \sigma (T_s + T_a) (T_s^2 + T_a^2) A_s (T_s - T_a) \tag{16}$$

The radiation heat transfer coefficient, $h_{radiation}$, is then defined as follows:

$$h_{radiation} = \sigma (T_s + T_a) (T_s^2 + T_a^2) \tag{17}$$

MODELING METHODOLOGY

As depicted in Fig. 1, the computational model is based on a one dimensional air flow pattern in which the air traverses the full length of the bulk load. In the computational model, the bulk load is represented as a porous medium composed of "commodity computational cells." The refrigerated air is modeled as "air parcels" which move through the "commodity computational cells."

Calculation commences with a specified initial temperature and humidity for the commodity bulk load and the air contained within it. As shown in Fig. 1a, the time-stepping begins with the first refrigerated "air parcel" moving into the first "commodity computational cell." At the same time, each of the initial "air parcels" moves from its original cell into the adjacent cell, while the "air parcel" within the last "commodity computational cell" moves from the bulk load into the plenum of the refrigeration unit. Within each "commodity computational cell," the commodity surface water vapor pressure, P_s, and air stream water vapor pressure, P_a, are determined based upon the commodity surface temperature, T_s, the "air parcel" temperature, T_a, and the "air parcel's" mass fraction of water vapor, m_f. These vapor pressures are then used to calculate the commodity transpiration, $\dot{m}$ 18, for the time-step, $?t$. The mass fraction of water vapor in each "air parcel" is then updated to reflect the effects of transpiration. Subsequently, within each cell, the heat generation due to commodity respiration, *W*, the heat transfer from the commodity, *Q*, and the evaporative cooling due to transpiration are calculated for the time-step. Then, within each cell, the commodity temperature and the "air parcel" temperature are both updated to reflect the effects of the calculated respiration, heat transfer and evaporative cooling, thus completing the calculations for this time-

step.

As shown in Fig. 1b, the first "air parcel" moves to the second "commodity computational cell" and a newly refrigerated second "air parcel" moves into the first "commodity computational cell." This second "air parcel" encounters the previously updated commodity temperature in the first "commodity computational cell."

As the time-stepping continues, each "air parcel" traverses the entire commodity bulk load. The mass fraction of water vapor contained in each "air parcel," when it exits the bulk load, is used to calculate the latent heat load corresponding to that "air parcel," while its temperature is used to calculate its sensible heat load. As this algorithm time-steps towards a steady state, an estimate of the time histories of the latent and sensible heat loads, as well as commodity moisture loss and temperature distribution, are obtained.

DESCRIPTION OF THE MASS AND HEAT TRANSFER MODELS

The modeling of the mass and heat transfer, between the air and the bulk load of commodities within a "commodity computational cell," is achieved by formulating the mass and heat transfer with

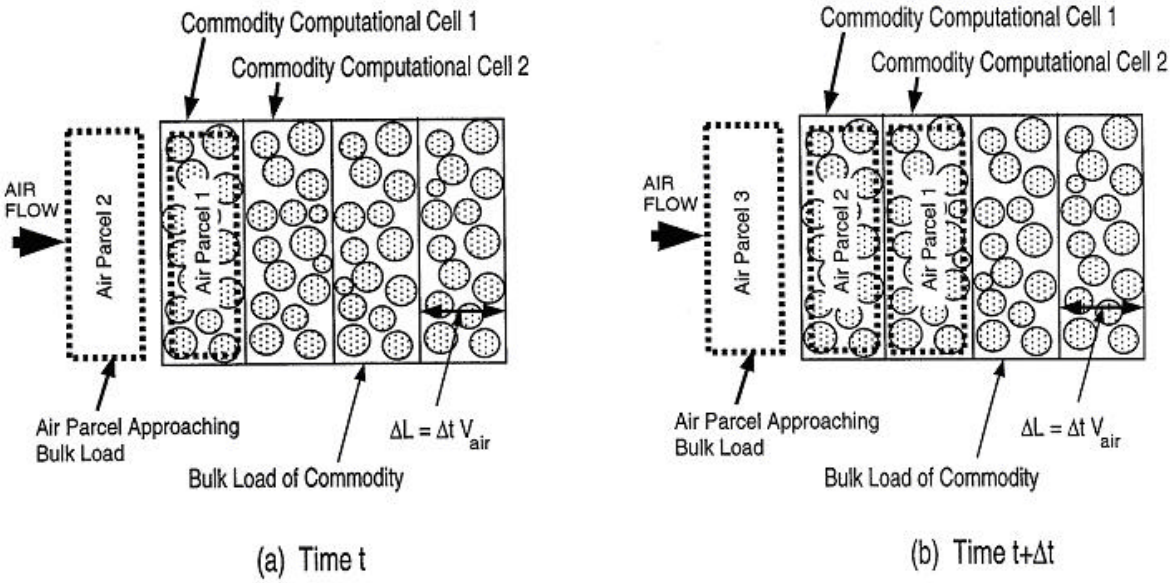

Figure 1. Computational model of refrigerated air flow through bulk load of commodity.

respect to a single commodity item, and then multiplying by the number of items resident within the "commodity computational cell."

Mass Transfer Calculation

The moisture loss from a single commodity item is modeled using Eq. 1 and Eq. 2. Both P_s and P_a are evaluated at the previous time step by utilizing Eq. 5 and Eq. 10. For one computational cell, the transpiration rate becomes:

$$\dot{m}_t = \dot{m}\ A_s\ n_c \tag{18}$$

where $\dot{m}_t$ 19 is the total transpiration rate in the computational cell, $\dot{m}$ 20 is the transpiration rate per unit

area of the commodity surface, A_s is the surface area of a single commodity item, and n_c is the number of commodities in the computational cell.

During the time step, $?t$, the mass of water vapor in the air of the computational cell increases as follows:

$$m_{H2O}^{1} = m_{H2O}^{0} + \dot{m}_t \Delta t \tag{19}$$

where m_{H2O}^{1} is the updated mass of water vapor in the air, m_{H2O}^{0} is the mass of water vapor in the air from the previous time step, $\dot{m}_t$ 20 is the transpiration rate and $?t$ is the time step size. The updated mass fraction of water vapor in the air of the computational cell, m_f^1, then becomes:

$$m_f^1 = \frac{m_{H2O}^{1}}{m_a^0 + \dot{m}_t \Delta t} \tag{20}$$

where m_a^0 is the mass of air in the computational cell at the previous time step. This completes the transpiration calculations for one computational cell for the current time step.

Heat Transfer Calculation

In order to make the modeling of the commodity heat transfer tractable, the commodities were assumed to be spherical in shape with uniform internal heat generation due to respiration. It was further assumed that the temperature within a commodity varied only in the radial direction. With these assumptions, the governing form of the transient heat equation is formally written as follows (Incropera and DeWitt, 1990):

$$\frac{k}{r^2}\frac{\partial}{\partial r}\left(r^2\frac{\partial T}{\partial r}\right) + \rho W = \rho c\frac{\partial T}{\partial t} \tag{21}$$

An explicit finite difference technique was applied to Eq. 21 by dividing a commodity into N spherical shells. The resulting finite difference equation applicable to the center node is given as follows:

$$\frac{k A_1}{\Delta r}(T_2^0 - T_1^0) + \rho v_1 W_1 = \frac{\rho c v_1 (T_1^1 - T_1^0)}{\Delta t} \tag{22}$$

For the interior nodes, the finite difference equation becomes:

$$\frac{k A_{i-1}(T_{i-1}^0 - T_i^0)}{\Delta r} + \frac{k A_i (T_{i+1}^0 - T_i^0)}{\Delta r} + \rho v_i W_i = \frac{\rho c v_i (T_i^1 - T_i^0)}{\Delta t} \tag{23}$$

At the surface of the commodity, convection heat transfer, radiation heat transfer, and evaporative cooling due to transpiration must be considered. Thus, the finite difference equation at the commodity surface becomes:

$$\frac{k A_{N-1}}{\Delta r}(T_{N-1}^0 - T_N^0) + h_{eff} A_s (T_a^0 - T_N^0) - L\dot{m} A_s + \rho v_N W_N = \frac{\rho c v_N (T_N^1 - T_N^0)}{\Delta t} \tag{24}$$

The formulation given by Eq. 22 through Eq. 24 defines the temperature distribution within a single commodity item. However, Eq. 24 requires knowledge of the temperature of the air parcel resident within the "commodity computational cell," T_a^0. This air temperature is determined at each time step by performing a heat balance between the air parcel and that portion of the bulk load which is contained within

the "commodity computational cell:"

$$n_c\, h_{eff}\, A_s (T_a^0 - T_N^0) = m_a^0\, c_{p,a} \frac{(T_a^1 - T_a^0)}{\Delta t} \tag{25}$$

where $c_{p,a}$ is the specific heat of air. This completes the formulation of the heat transfer model for one computational cell.

Since Eq. 22 through Eq. 25 are explicit finite difference equations, they can be solved directly for the updated nodal temperatures. The heat transfer calculation begins at the commodity center node and proceeds outward to the air parcel. This completes the heat transfer calculation for one computational cell for the current time step.

EXPERIMENTAL VERIFICATION OF THE COMPUTER ALGORITHM

To verify the accuracy of the current computer algorithm, its calculated results were compared with experimental data obtained from the literature. Baird and Gaffney (1976) reported experimental data taken from bulk loads of oranges. They recorded commodity center and surface temperatures at the air exit of a bulk load for a period of two hours. The bulk load of oranges was 0.67 m (2.2 ft) deep and the commodities were initially at 32°C (90°F). The refrigerated air was at a temperature of -1.1°C (30°F) and approached the bulk load with a velocity of 0.91 m/s (3.0 ft/s). Figure 2 shows Baird and Gaffney's experimental data along with the output from the current computer algorithm. Comparison of the model results with Baird and Gaffney's data on oranges shows that the current algorithm correctly predicts the trends of commodity temperatures with a maximum error of 1.4°C (2.5°F).

Gan and Woods (1989) gathered experimental data on swedes (rutabagas) during cooling in a thin bed. Air at 4.96°C (40.9°F), 83.71% relative humidity flowed at a velocity of 0.53 m/s (1.7 ft/s) through a bed of swedes which was initially at a temperature of 21.7°C (71.1°F). Commodity center temperature and moisture loss were recorded for a period of eight hours. Figure 3 shows the Gan and Woods temperature data along with the output from the current algorithm, while Fig. 4 shows the Gan and Woods moisture loss data along with the output from the current algorithm. It is seen that the current algorithm correctly predicts commodity temperatures within 2.2°C (4.0°F) and moisture loss within 0.38%.

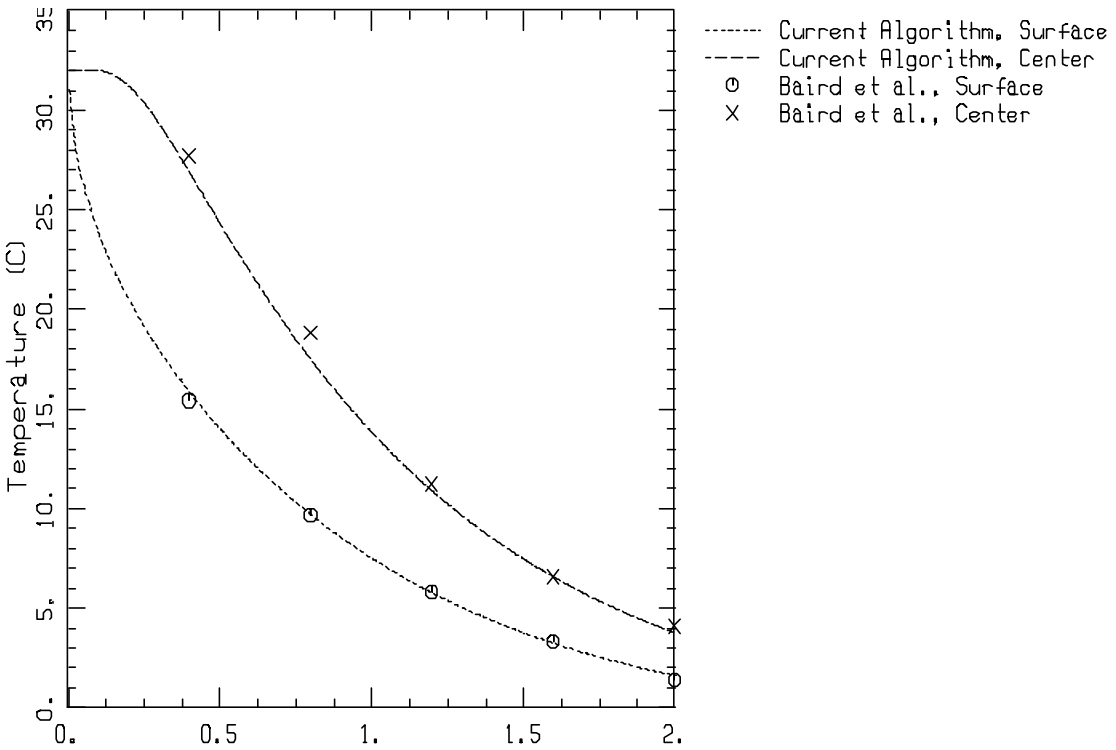

Figure 2. Current numerical results and experimental data on oranges from Baird and Gaffney (1976).

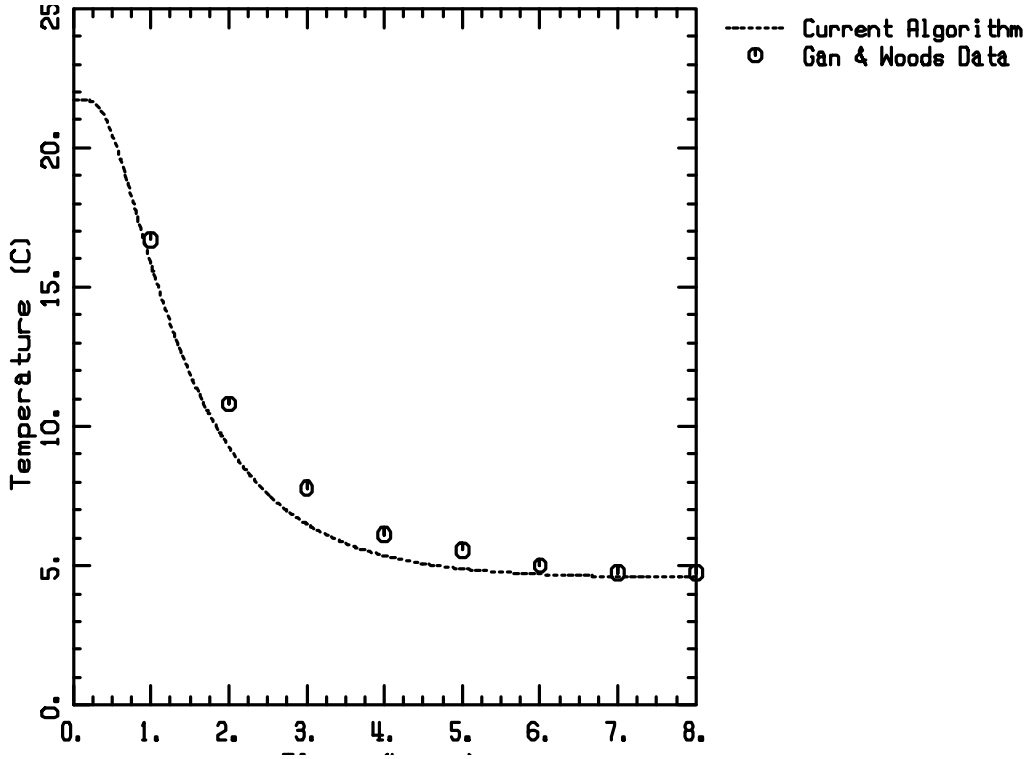

Figure 3. Current numerical results and experimental data on swedes from Gan and Woods (1989).

Güemes et al. (1989) collected temperature data for the cooling of strawberries in a thin bed. Air with a velocity of 3.0 m/s (9.8 ft/s) and a temperature of 2.1°C (36°F) was used to cool the strawberries for a period of 16 minutes. As shown in Fig. 5, the output from the current algorithm compares favorably with the data from Güemes et al. The maximum error between the computer algorithm and the experimental results was 1.9°C (3.4°F).

CONCLUSIONS

This paper has described the development and performance of a computer algorithm which estimates the latent and sensible heat loads as well as the moisture loss and temperature distribution in the bulk refrigeration of fruits and vegetables. This algorithm, which was developed as an aid to both the designer and the operator of refrigeration facilities, is capable of modeling a wide variety of commodities. In addition, this paper described the thermophysical properties of commodities and the flowfield parameters which govern the heat and mass transfer from fresh fruits and vegetables.

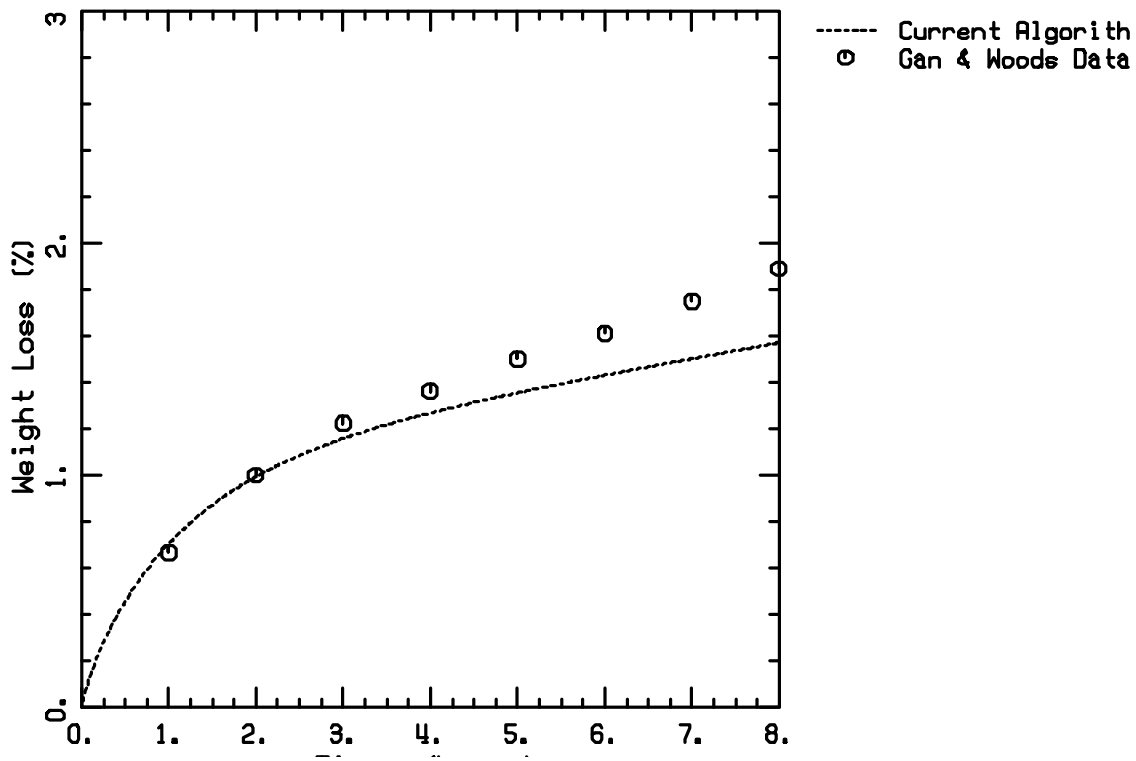

Figure 4. Current numerical results and experimental data on swedes from Gan and Woods (1989).

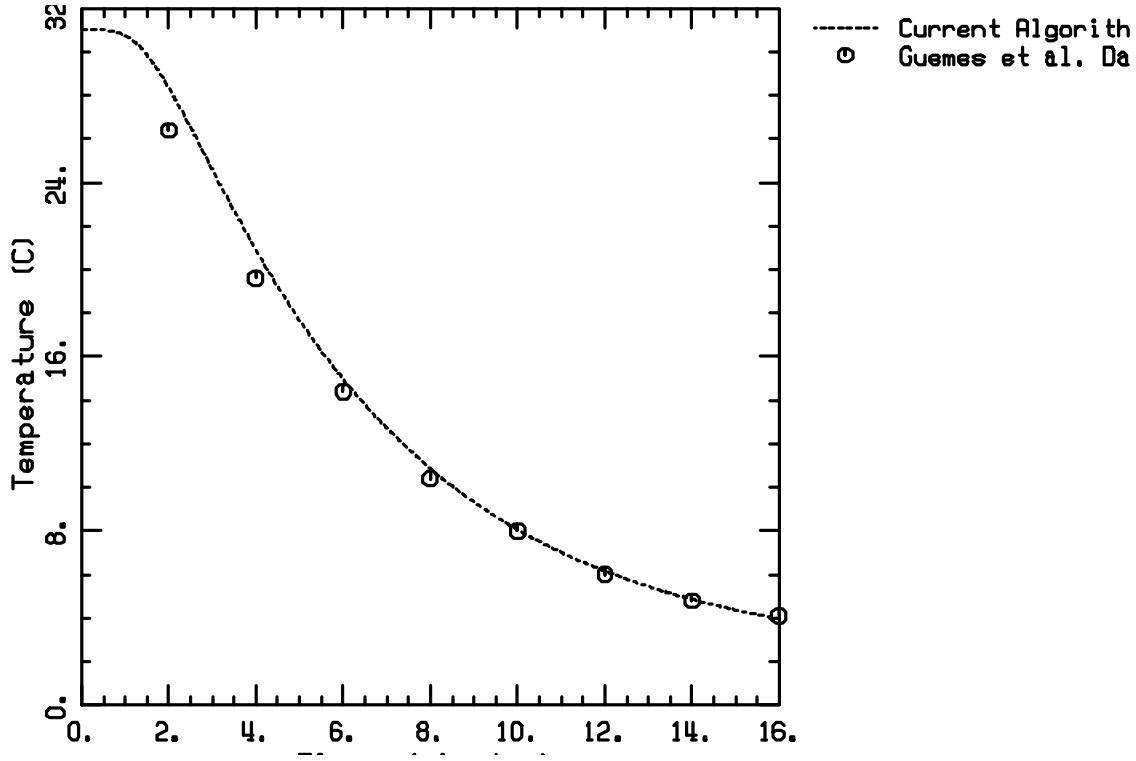

Figure 5. Current numerical results and experimental data on strawberries from Güemes et al. (1989).

A mathematical model for transpiration was identified which utilizes a variable transpiration coefficient consisting of an air film mass transfer coefficient and a skin mass transfer coefficient. A Sherwood-Reynolds-Schmidt correlation was given for the air film mass transfer coefficient while values of the skin mass transfer coefficient for various commodities were tabulated. In addition, the vapor pressure lowering effects of various commodities were tabulated from published data.

A model was developed which relates respiratory heat generation to commodity temperature via carbon dioxide production. Empirical correlations were developed and presented which relate the carbon dioxide production of various commodities to their temperature.

Psychrometric functions were given for the calculation of the water vapor pressure in the refrigerated air and at the commodity surface. A Nusselt-Reynolds-Prandtl correlation was given for the convection heat transfer coefficient. An expression for the radiation heat transfer coefficient as a function of temperature was derived. An effective heat transfer coefficient was defined as the sum of the convection and radiation heat transfer coefficients.

This paper described the modeling methodology which was devised for studying the mass and heat transfer processes within a bulk load of commodities. In the computational model, the bulk load is represented as a porous medium composed of "commodity computational cells" and the refrigerated air is modeled as "air parcels" which move through these "commodity computational cells." The modeling of the mass and heat transfer between the air and the bulk load is achieved by formulating the mass and heat transfer with respect to a single commodity item and then multiplying by the number of items resident within the "commodity computational cell."

A mass transfer model was developed to update the mass fraction of water vapor within each "commodity computational cell" at each time step based upon the transpiration model identified in the literature. An explicit finite difference formulation of the transient heat equation in spherical coordinates was derived which accounts for both radiation and convection heat transfer at the commodity surface. This formulation yields the temperature distribution within the commodities resident in each "commodity computational cell" at each time step. It also yields the temperature of the "air parcel" resident within each "commodity computational cell" at each time step.

To verify the accuracy of the current algorithm, its calculated results were compared with experimental data obtained from the literature. The results of the heat transfer model were compared to experimental temperature data for oranges, swedes and strawberries, while the results of the mass transfer model were compared to experimental moisture loss data for swedes. The results of these comparisons show good agreement between the numerical results and the experimental data for both temperature and moisture loss.

NOMENCLATURE

A_1	surface area of center node
A_i	surface area of i^{th} node
A_s	single commodity surface area
c	specific heat of commodity
$c_{p,a}$	specific heat of air
d	diameter of fruit or vegetable
f	carbon dioxide production vs. temperature correlation coefficient
g	carbon dioxide production vs. temperature correlation coefficient
$h_{convection}$	convection heat transfer coefficient
h_{eff}	effective heat transfer coefficient
$h_{radiation}$	radiation heat transfer coefficient
k	thermal conductivity of commodity
k_a	air film mass transfer coefficient
k_{air}	thermal conductivity of air
k_s	skin mass transfer coefficient
k_t	transpiration coefficient
L	latent heat of vaporization of water
m_a^0	mass of air at time t
m_f	mass fraction of water vapor in air
m_f^1	mass fraction of water vapor in air at time $t + ?t$
m_{H2O}^0	mass of water vapor in air at time t
m_{H2O}^1	mass of water vapor in air at time $t + ?t$
$\dot{m}$	transpiration rate per unit area of commodity surface
$\dot{m}_{CO2}$	carbon dioxide production rate
$\dot{m}_t$	transpiration rate in computational cell
N	number of commodity shells
n_c	number of commodities in computational cell
Nu	Nusselt number
P	atmospheric pressure
P_a	ambient water vapor pressure
P_s	water vapor pressure at evaporating surface of commodity
$P_{ws}(T)$	water vapor saturation pressure evaluated at temperature T
Pr	Prandtl number
Q	heat transfer
Q_r	radiation heat transfer
r	commodity radius
Re	Reynolds number
Sc	Schmidt number
Sh	Sherwood number
t	time
T	commodity temperature
T_1^0	temperature of center node at time t
T_1^1	temperature of center node at time $t + ?t$
T_a	dry bulb air temperature
T_a^0	air temperature at time t
T_a^1	air temperature at time $t + ?t$
$T_{a,absolute}$	dry bulb air temperature in absolute degrees (K)
T_i^0	temperature of i^{th} node at time t
T_i^1	temperature of i^{th} node at time $t + ?t$
T_m	mass average temperature of commodity
T_N^0	temperature of surface node at time t
T_N^1	temperature of surface node at time $t + ?t$
T_s	product surface temperature
$u_¥$	free stream air velocity
v_1	volume of center node
v_i	volume of i^{th} node
v_N	volume of surface node
VPL	vapor pressure lowering effect
w	humidity ratio
W	rate of respiratory heat generation of commodity per unit mass of commodity
W_1	rate of respiratory heat generation of commodity per unit mass of commodity for center node

W_i	rate of respiratory heat generation of commodity per unit mass of commodity for node i
W_N	rate of respiratory heat generation of commodity per unit mass of commodity for surface node
a	thermal diffusivity of commodity
d	coefficient of diffusion of water vapor in air
$?r$	length of node in radial direction
$?t$	time step size
$?$	dimensionless temperature ratio
v	kinematic viscosity of air
$?$	density of commodity
s	Stefan-Boltzmann constant

REFERENCES

1. Adre, N., and M.L. Hellickson. 1989. Simulation of the Transient Refrigeration Load in a Cold Storage for Apples and Pears. *Transactions of the ASAE* 32(3): 1038-1048.
2. ASHRAE. 1977. *Brochure on Psychrometry*. Atlanta: ASHRAE.
3. ASHRAE. 1993. *1993 ASHRAE Handbook -- Fundamentals*. Atlanta: ASHRAE.
4. Baird, C.D., and J.J. Gaffney. 1976. A Numerical Procedure for Calculating Heat Transfer in Bulk Loads of Fruits or Vegetables. *ASHRAE Transactions* 82(2): 525-540.
5. Bakker-Arkema, F.W., and W.G. Bickert. 1966. A Deep-Bed Computational Cooling Procedure for Biological Products. *Transactions of the ASAE* 9(6): 834-836, 845.
6. Chau, K.V., R.A. Romero, C.D. Baird, and J.J. Gaffney. 1987. Transpiration Coefficients of Fruits and Vegetables in Refrigerated Storage. *ASHRAE Report 370-RP*. Atlanta: ASHRAE.
7. Fockens, F.H., and H.F.T. Meffert. 1972. Biophysical Properties of Horticultural Products as Related to Loss of Moisture During Cooling Down. *Journal of the Science of Food and Agriculture* 23: 285-298.
8. Gan, G., and J.L. Woods. 1989. A Deep Bed Simulation of Vegetable Cooling. In *Agricultural Engineering*, ed. V.A. Dodd and P.M. Grace, pp. 2301-2308. Rotterdam: A.A. Balkema.
9. Geankoplis, C.J. 1978. *Transport Processes and Unit Operations*. Boston: Allyn and Bacon.
10. Güemes, D.R., M.E. Pirovani, and J.H. Di Pentima. 1989. Heat Transfer Characteristics During Air Precooling of Strawberries. *International Journal of Refrigeration* 12(3): 169-173.
11. Incropera, F.P., and D.P. DeWitt. 1990. *Fundamentals of Heat and Mass Transfer*. New York: John Wiley and Sons.
12. MacKinnon, I.R., and W.K. Bilanski. 1992. Heat and Mass Transfer Characteristics of Fruits and Vegetables Prior to Shipment. *SAE Technical Paper 921620*. Warrendale, PA: SAE.
13. Sastry, S.K., C.D. Baird, and D.E. Buffington. 1978. Transpiration Rates of Certain Fruits and Vegetables. *ASHRAE Transactions* 84(1): 237-254.
14. Sastry, S.K., and D.E. Buffington. 1982. Transpiration Rates of Stored Perishable Commodities: A Mathematical Model and Experiments on Tomatoes. *ASHRAE Transactions* 88(1): 159-184.
15. Talbot, M.T., C.C. Oliver, and J.J. Gaffney. 1990. Pressure and Velocity Distribution for Air Flow Through Fruits Packed in Shipping Containers Using Porous Media Flow Analysis. *ASHRAE Transactions* 96(1): 406-417.
16. USDA. 1986. *The Commercial Storage of Fruits, Vegetables, and Florist and Nursery Stocks, Agricultural Handbook Number 66*, United States Department of Agriculture.